17th Brazilian Congress of Thermal Sciences and Engineering
November 25th-28th, 2018, Águas de Lindóia, SP, Brazil

ENCIT-2018-0511

EXPERIMENTAL STUDY OF HYDRATE FORMATION IN NON EMULSIFYING OIL SYSTEMS IN SHUT-IN AND RESTART CONDITIONS

Celina Kakitani - ckakitani@gmail.com
Moisés A. Marcelino Neto - mneto@utfpr.edu.br
Rigoberto E. M Morales - rmorales@utfpr.edu.br
Multiphase Flow Research Center - NUEM
Federal University of Technology - Parana (UTFPR)
5000 Deputado Heitor Alencar Furtado Street, Curitiba, Parana, Brazil

Amadeu K. Sum - asum@mines.edu
Hydrates Energy Innovation Lab.
Colorado School of Mines
1500 Illinois Street, Golden, Colorado, USA

Abstract. *Gas hydrates are crystalline structures formed by water and gas molecules at high pressure and/or low temperature. Formation of hydrate blockages represents both an economical loss and a safety concern in operation of a pipeline. For oil and gas industry, hydrate plug formation is one of the most concerns in flow assurance. Transient operations, involving shut-in and restart is the most challenging scenario with risk for hydrate problems. Cooling of the stagnant fluid in the line due to thermal exchange with the seabed may cause the pressure and temperature conditions to enter the hydrate forming zone. The restart could result in a rapid hydrate formation and even form hydrate plug. This work is focused on studying the behavior of hydrate formation in transient conditions. Experiments were performed in a high pressure cell coupled in a rheometer using a custom-designed impeller with a three-phase system of gas, liquid hydrocarbon and aqueous phase. The influence on hydrate formation and restart were studied with respect to rotational speed, pressure and subcooling. The effects of adding a commercial anti-agglomerant (AA) were also studied in some of the experiments. It was observed that these parameters could influence the hydrate crystal morphology.*

Keywords: *gas hydrate, rheometer, shut-in/restart*

1. INTRODUCTION

The increasing demand for fossil fuel has generated the need to explore fields under more severe conditions, such as the pre-salt (Sloan, 2003). Due to the gas and oil production in deeper water scenarios, the concerns about precipitation of solids, such as wax and asphaltene, solid deposition, such as sand, and scale and hydrate formation are increasing (Oliveira *et al.*, 2011 and Webb *et al.*, 2014). Most of these phenomena take time to blockage the line unlike the hydrate plug formation which can form very quickly at right conditions (Sloan *et al.*, 2011).

Gas hydrates are crystalline structures composed by water and gas molecules formed under conditions of low temperature and/or high pressure. The hydrate plug can rupture the flowline through projectile impact and it can involve safety concerns in the field. The petroleum industry adopts some strategies to avoid the hydrate formation (thermodynamic and kinetic inhibitors, for instance) or let the hydrate in flowable conditions (anti-agglomerant inhibitor – AA). The inhibitors cost for the petroleum industry thousands of dollars per day (Creek *et al.*, 2011). Besides the high cost, the inhibiting procedures are time-consuming resulting in loss of production, in addition to presenting operational risk.

In the flow assurance of oil and gas production systems, transient operation involving shut-in and restart is the most challenging scenario with risk for hydrate problems. During the shut-in, the fluids are stationary and are quickly cooled down due to heat transfer with the subsea environment. Therefore, depending on the shut-in time, fluids can enter in the hydrate zone, which upon restart could result in rapid hydrate formation possibly leading to a plug or severe restriction.

This work is focused on understanding the behavior of hydrate formation in transient condition and identifying which conditions hydrate plugs form or flowable conditions results with the restart. Experiments were performed in a high pressure cell coupled with the rheometer. It was analysed the influence of variables such as pressure, temperature, rotational speed after a simulation of long period of shut-in. Also, two different anti-agglomerants were added in the system in order to check their efficiency. Knowing the parameters that influence the formation of hydrates and the involved phenomena are important to develop and improve techniques of inhibition of hydrate plug formation in transient regime.

2. EXPERIMENTAL SETUP

Figure 1 shows a schematic experimental setup which was composed by the gas cylinder (a), the syring pump (b) (Teledyne Isco, model 200DM) which controlled the pressure and gas feed to the cell, the chiller (c) which was responsible for the temperature control of the cell, the high pressure cell (d) coupled with the rheometer (Discovery Hybrid Rheometer – 2 from TA Instruments) which was responsible for torque measurements. The maximum volume of the cell was 35 ml and the operating pressure was up to 100 bar. The pressure cell interior dimensions were 57 mm in height and 28 mm in diameter. The impeller used was custom made with 1 mm of gap from outer vane to the cell wall in order to avoid accumulation of hydrate at the wall and in the middle section. The impeller dimensions were 40 mm in height and 26 mm in diameter.

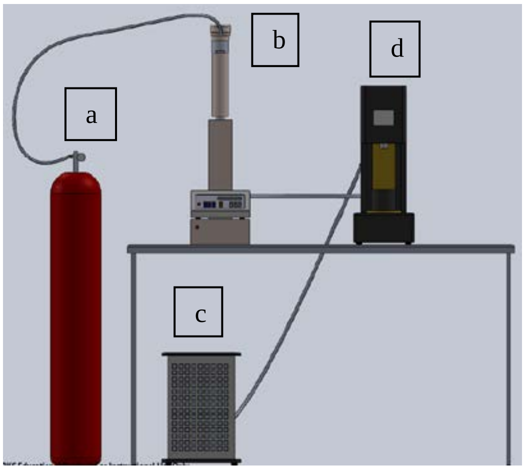

Figure 1 Schematic of the rheometer apparatus.

Experiments were performed at constant pressure (method isobaric) using three phases: deionized water, mineral oil 70T (purchased from STE Oil Company, Inc.) and gas mixture (approximately 92 mol % methane and 8 mol % propane). The liquid loading was 25 ml with different amounts of water cut (10%, 30% and 50%) and two different commercial AAs (named AA-01 and AA-02) were used in the experiments.

3. METHODOLOGY

The experiment preliminary steps started with cleaning of the cell with water and dish cleaning soap followed by a throughout rinsing with deionized water. Then, the experiment started with the rheometer calibration with the cell empty. The liquids (hydrocarbon phase and aqueous phase) were filled by weight under atmospheric conditions and the cell was pressurized until the pressure of the experiment desired was achieved. After verifying the absence of gas leakage, the experiment started at 25ºC.

Two different experimental procedures were used in this work. One of them consists in 4 steps: (1) Gas saturation: when the gas flow rate between the syringe pump and the cell was zero, it indicated that the liquid was saturated. (2) Hydrate formation: the set point temperature of the chiller was changed from 25ºC to the experimental temperature for the given experiment and it was kept at this temperature throughout the experiment. (3) Shut-in: when the measure of torque was stable and the gas flow rate was zero, the system achieved the steady-state, then the system was kept quiescent for several hours. (4) Restart: the same rotational speed before shut-in was applied. The experiment was finished when the steady-state was achieved.

The second procedure consists in six steps: (1) Gas saturation: this step was the same as described in the previous procedure. (2) Cooling down: the set point temperature of the chiller was changed from 25ºC to the experimental temperature for the given experiment in steps (4 ºC/h) in a low rotational speed (5 rpm) in order to avoid hydrate formation in this step. (3) First shut-in: this step was the same as described in the previous procedure. (4) First restart: the same rotational speed as the saturation step was applied and hydrate formation occurred in this step. (5) Second shut-in: after the steady-state was achieved in the previous step, which means stable torque and gas flow rate equal zero, the system was kept quiescent for several hours. (6) Second restart: in order to analyze the behavior result with the restart with hydrate in the system, the same rotational speed used in step 4 was applied. The experiment was finished when the steady-state was achieved. Therefore, experiments with varying rotational speed were performed in order to study the influence of the rotational speed in the hydrate structure.

Torque and the change in the syringe pump volume due hydrate formation were recorded throughout the experiments. However, the custom-designed hollow vane results in an undefined shear which means unknown viscosity. Charin and Sum (2017) found some correlations to convert the measured torque for the geometry used to known viscosity fluids. In this work, it was used the same correlations as Charin and Sum (2017). Assuming a hydration number of 6 mol of water/ mol of gas, the volume variation in the pump was used to estimate the volume of hydrate formed and the hydrate fraction relative to the total liquid volume.

4. RESULTS

This study seeks to understand the rheological properties of hydrate slurry in transient conditions. In order to study the hydrate formation behavior, experiments were performed using different water cut (10%, 30% and 50%), different impeller rotational speed and two different commercial anti-agglomerants. Figure 2 shows the apparent viscosity (converted from the torque) and hydrate fraction (calculated from the volume variation in the syringe pump) versus time for a blank test, which means without AA. The first procedure described in Section 3 was used in this experiment. The rotational speed of this experiment was 200 rpm, 10% of water cut, at 1000 psig, 18ºC of subcooling and a three phase system: deionized water as aqueous phase, mineral oil as oil phase and gas mixture (methane and propane) as gas phase.

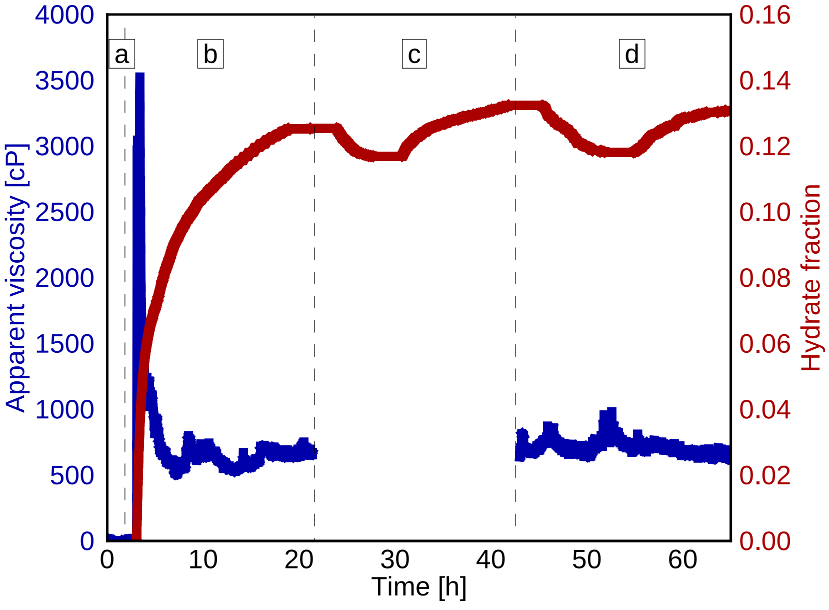

Figure 2 Typical experiment showing the stages: (a) gas saturation; (b) hydrate formation; (c) shut-in and (d) restart.

Figure 2 shows a typical experiment which was divided in some stages: (a) saturation; (b) hydrate formation; (c) shut-in and (d) restart. The presence of a significant amount of hydrate was detected with the suddenly increase of the apparent viscosity. Webb et al. (2014) attribute the accentuated increase of the viscosity due to the response to the conversion of liquid water into solid particles of hydrate, and also by the dissolution and depletion of the gas in the oil phase, by the agglomeration of the solid particles and by capillary connections. The viscosity drop shortly after the peak indicated the hydrate formation due to the alignment of the particles in the flow (Quemada, 1978, Webb et al., 2014). After a period of time, the steady state was achieved. At this point, the mixing was stopped and the system was remained quiescent for several hours in order to simulate the shut-in in the line. Hence the system was restarted and the apparent viscosity monitored to determine the state of the system. In most of the experiments the apparent viscosity on restart and before shut-in were equivalents, showing a viscoelastic behavior.

Figure 3 shows the apparent viscosity and the hydrate fraction for a 30% water cut experiment with mineral oil and 1 wt% AA-01. The second procedure described in Section 3 was used in this experiment, until step (4). Figure 3 shows the stages: (a) cooling at 5 rpm; (b) shut-in and (c) restart at 200 rpm. This experiment was performed using AA and it had the same behavior as the blank test.

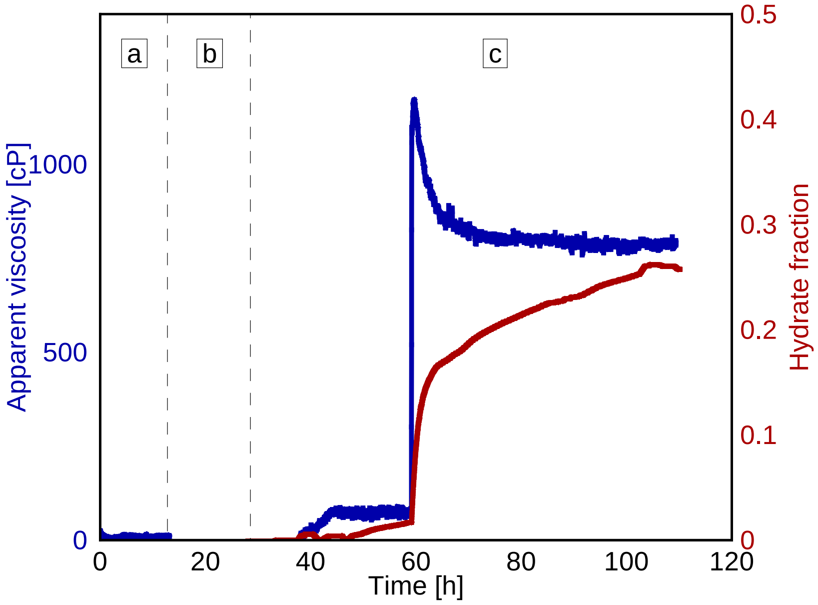

Figure 3 Experiment using mineral oil and AA-01. Stages: (a) cooling; (b) shut-in; (c) restart.

Figure 4 shows a result from an experiment varying rotational speed using the first protocol described in Section 3. The sequence of rotational speeds was (a) saturation at 200 rpm; (b) cooling and hydrate formation at 200 rpm; (c) 100 rpm; (d) 200 rpm; (e) 300 rpm; (f) 200 rpm, (g) shut-in and (f) restart at 200 rpm. This was a blank test with 10% of water cut, at 1000 psig and 18ºC of subcooling.

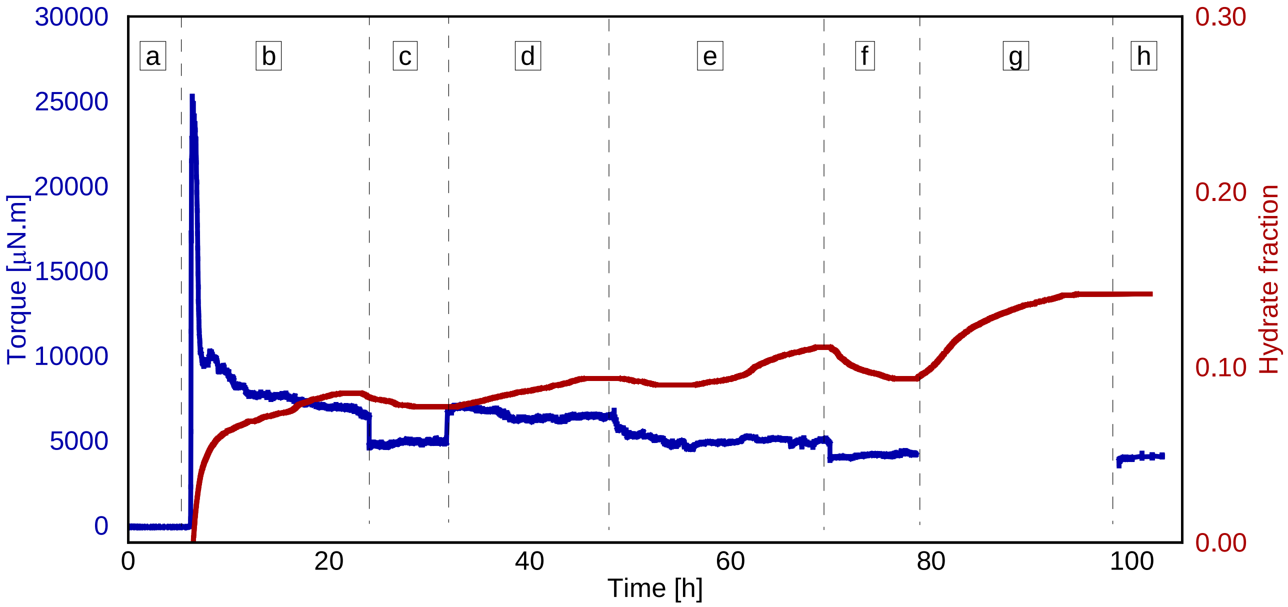

Figure 4 Torque /hydrate fraction versus time – (a) saturation; (b) hydrate formation; (g) shut-in; (h) restart. Rotational speed: (b) 200 rpm; (c) 100 rpm; (d) 200 rpm; (e) 300 rpm; (f) 200 rpm; (h) 200 rpm.

It was observed from the experiment showed in Figure 4 that the rate of rotational speed can influence the structure of the hydrate. The increase in the rotational speed could cause the breakage of the hydrate structure. However for the decrease of the rotational speed, no change in the torque values was observed.

Figure 5 shows a result from an experiment varying rotational speed for a 50% water cut experiment with mineral oil and AA-01. The sequence of rotational speeds was (a) saturation at 200 rpm; (b) cooling at 5 rpm; (c) shut-in; (d) restart at 200 rpm; (e) 100 rpm; (f) 200 rpm; (g) 300 rpm; (h) 200 rpm, (i) shut-in and (j) restart at 200 rpm.

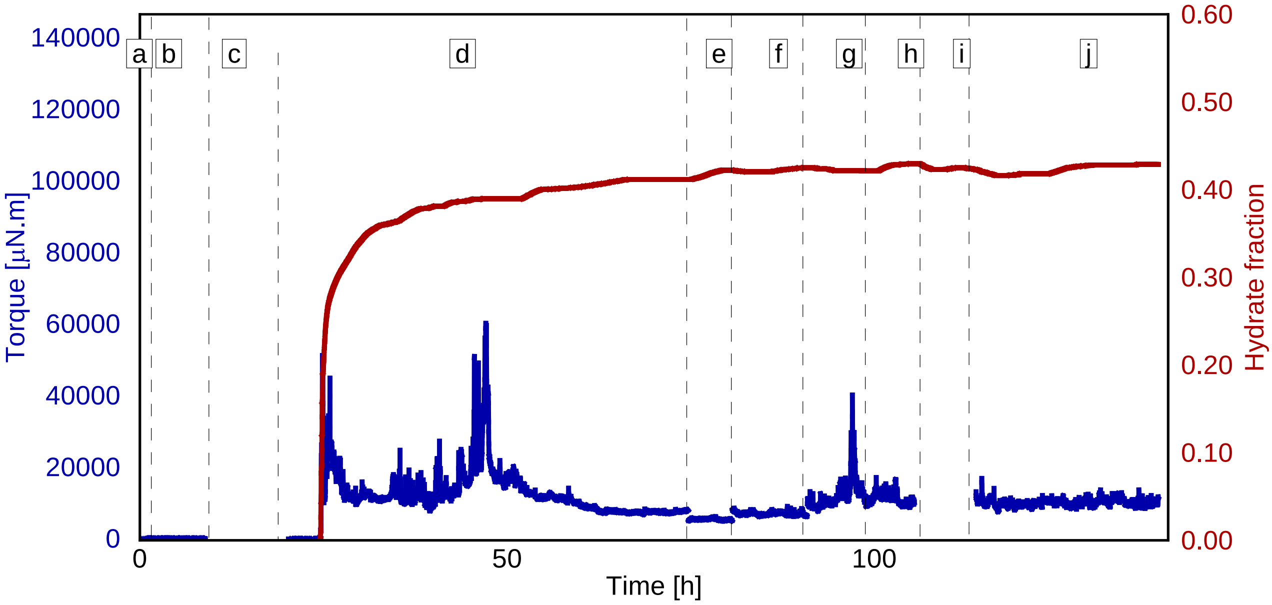

Figure 5 Torque /hydrate fraction versus time – (a) saturation; (b) cooling at 5 rpm; (c) shut-in; (d) restart at 200 rpm; (e) 100 rpm; (f) 200 rpm; (g) 300 rpm; (h) 200 rpm; (i) shut in and (j) restart at 200 rpm.

The decrease of the rotational speed did not change the torque values in Figure 4 and Figure 5. However, the increase in the rotational speed could help the hydrate agglomeration in Figure 5. This behavior was the opposite that was observed in Figure 4. One hypothesis is increasing the rotational speed, the AA efficiency could decrease and more hydrate agglomerated.

Figure 6 shows a result from an experiment varying rotational speed for a 50% water cut experiment with mineral oil and AA-02. Figure 6 shows the stages: (a) shut-in; (b) restart at 200 rpm; (c) shut-in; (d) restart at 200 rpm; (e) 100 rpm; (f) 200 rpm; (g) 300 rpm; (h) 200 rpm, (i) shut-in and (j) restart at 200 rpm. Two stages are not showed in Figure 6: saturation and cooling. In this case, the AA was efficient, keeping the hydrate particle dispersed, however the torque measured throughout the experiment was oscillating. It can be suggested that some chunks of hydrates were formed.

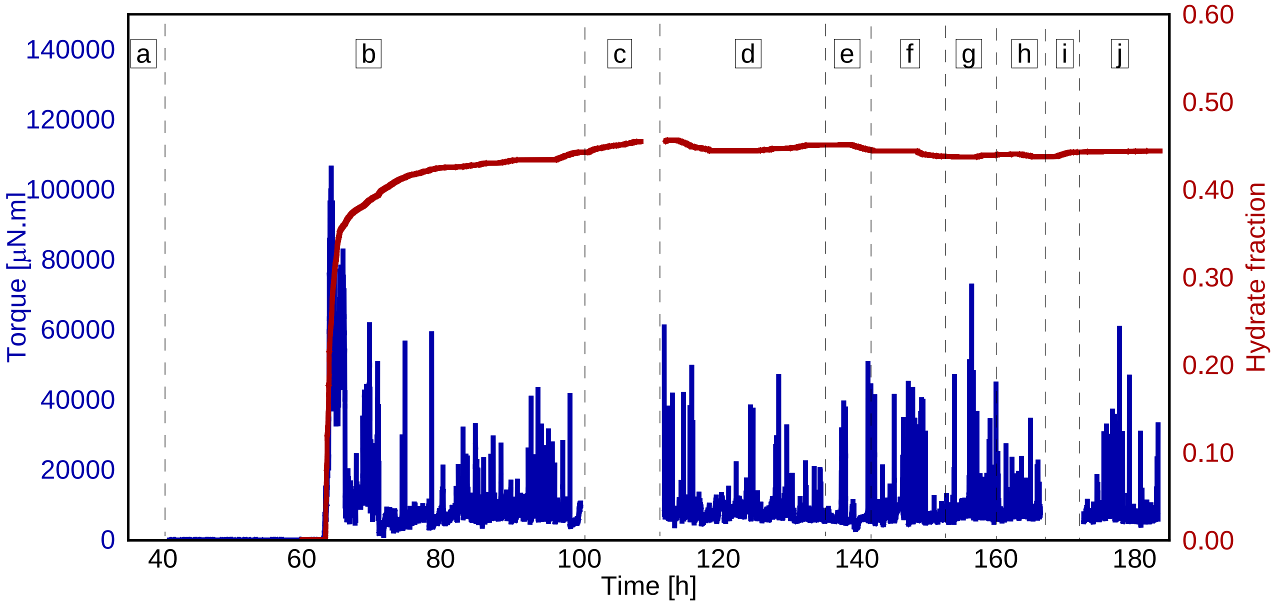

Figure 6 Torque /hydrate fraction versus time – (a) shut-in; (b) restart at 200 rpm; (c) shut-in; (d) restart at 200 rpm; (e) 100 rpm; (f) 200 rpm; (g) 300 rpm; (h) 200 rpm; (i) shut-in (j) restart at 200 rpm.

Experiments with 30% water cut were performed with and without AA which are shown in Figure 7. For the blank test, the experiment could not finish because the hydrate jammed during the formation and the torque increased above the instrument limit. The experiments with AA and 30% water cut formed a flowable slurry. Therefore, both AA's tested were efficient. As seen in Figure 7, the apparent viscosity measured for the experiments using AA-02 were higher than the experiments using AA-01. Considering the hydrate fraction formed in the experiments with AAs were close, it can be suggested that AA -01 formed hydrate particles better dispersed.

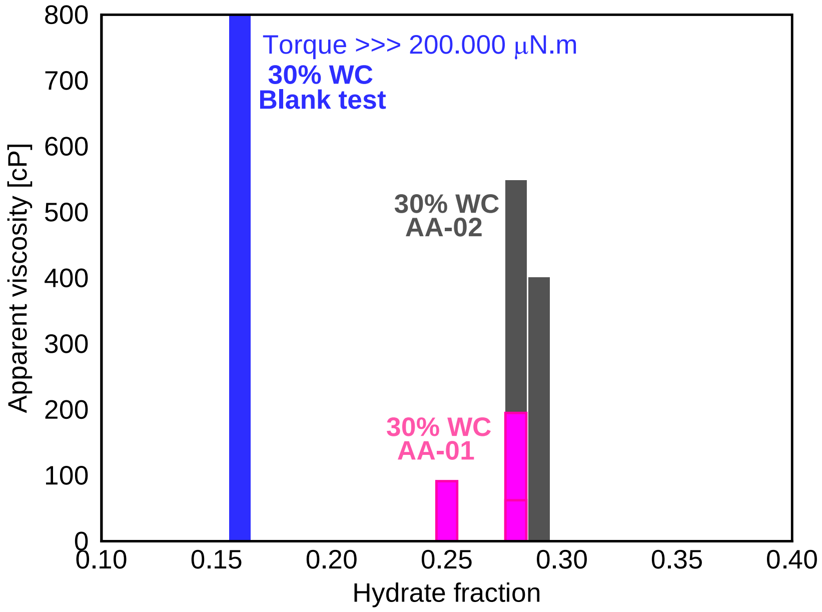

Figure 7 Apparent viscosity over hydrate fraction for experiments with 30% water cut.

Figure 8 correlates hydrate fraction to apparent viscosity for different water cuts. The higher water cuts produced more hydrates and it was consistent, as seen in the figure. It was tested two commercial AAs, which worked well and dispersed the hydrate particles. The experiments with AA-01 formed hydrate particles homogeneous and well dispersed, instead of the experiments with AA-02, which formed chunks of hydrates particles.

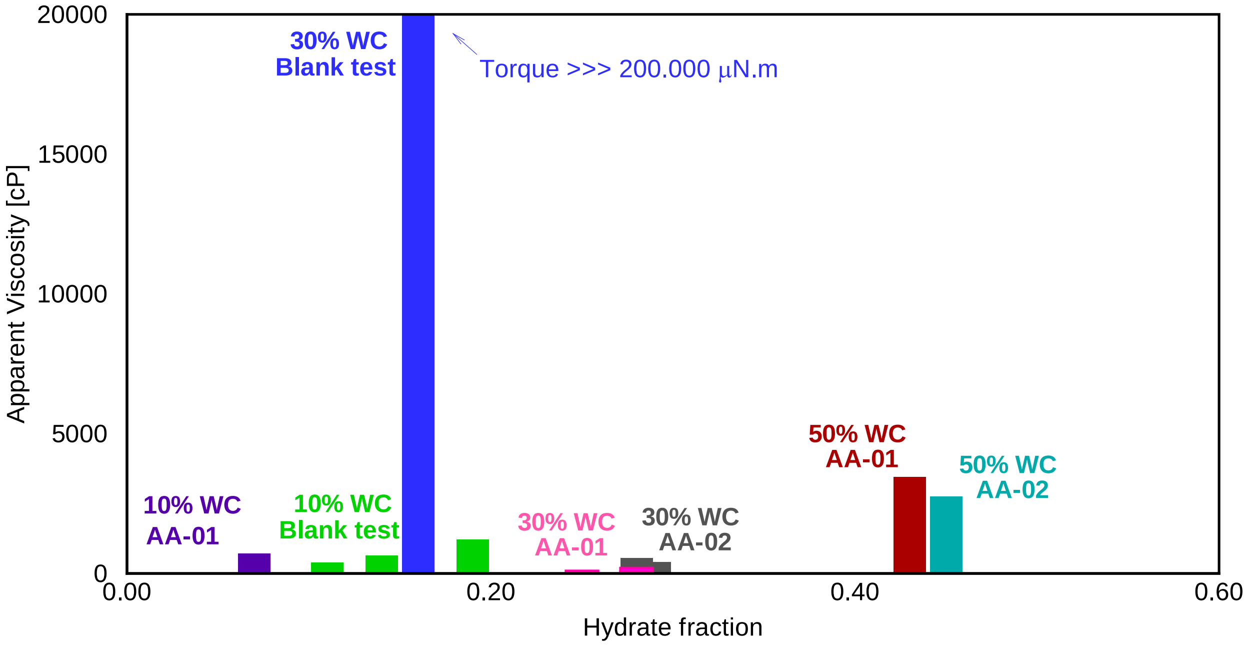

Figure 8 Apparent viscosity over hydrate fraction for all experiments.

5. CONCLUSIONS

Transient operations, such as in the case of a scheduled or emergency shutdowns, can result in conditions with a higher potential for hydrate plugs formation. Understanding and identifying which conditions hydrate plugs form or flowable conditions results with the restart can void some issues like blockage of the line. Many variables can influence the dynamics of hydrate formation in transient conditions, such as water cut, memory effect, viscosity of the oil phase, pressure, subcooling, emulsion stability, and shear/mixing at restart. For the experiments varying the rotational speed, it was observed that the increase in the rotational speed may cause the breakage of the hydrate structure due to the increase of the shear, and a decrease in the rotational speed does not recover the hydrate particle size as before the increase in the rotational speed.

Experiments with the AAs showed the efficiency of both of them even for 50% of water cut. Which means they dispersed the hydrates in the liquid phase. AA-01 was better, which means at the same system, the apparent viscosity was lower than the experiments with AA-02. In addition, blank tests with 30% of water cut or more were not possible to perform due the torque measure limitation of the rheometer.

In summary, the rheology of hydrate formation highly dependent on geometry, rotational speed, amount of water and the fluids. In addition, the rheology of hydrate can provide some useful qualification of AAs (which AA forms hydrate particle well dispersed).

6. ACKNOWLEDGEMENTS

The authors would like to thank the support of TE/CENPES/PETROBRAS, PRH-10 ANP and UTFPR.

7. REFERENCES

Charin, R.M.; Sum, A.K., 2017. “Steady-state and transient studies of gas hydrates formation in non-emulsifying oil systems”. *Energy & Fuels*, Vol. 31, p. 2548-2556.

Creek, J.L., Subramanian, S., Estanga, D., 2011. “New method for managing hydrates in deepwater tiebacks”. *Offshore Techonology Conference – OTC*, Houston, Texas, USA.

Quemada, D., 1978. “Rheology of concentrated disperse systems II. A model for non-newtonian shear viscosity in steady flows”. *Rheologica Acta*, Vol. 17, p. 632-642.

Oliveira, M.C.K., Teixeira, A., Vieira, L.C., Carvalho, R.M., Carvalho, A.B.M., Couto, B.C., 2011. “Flow assurance study for waxy crude oils”. *Energy Fuels*, Vol. 26, p. 2688-2695.

Sloan, D., Koh, C., Sum, A.K., 2011. “Natural gas hydrates in flow assurance”. Gulf Professional Publishing, Burlington, MA, 1st edition.

Sloan Jr., E.D., 2003. “Fundamental principles and application of natural gas hydrates”. *Nature*, Vol. 426, p. 353-359.

Webb, E.B., Koh, C.A., Liberatore, M.W., 2014. “High pressure rheology of hydrate slurries formed from water-in-mineral oil emulsions”. *Industrial & Engineering Chemistry Research*, Vol 53, p. 6998-7007.

8. RESPONSIBILITY NOTICE

The authors are the only responsible for the printed material included in this paper.